

Testing the Early Mars H₂-CO₂ Greenhouse Hypothesis with a 1-D Photochemical Model

Natasha Batalha^{a,b,c,**}, Shawn D. Domagal-Goldman^{c,d}, Ramses Ramirez^{e,f,g},
James F. Kasting^{b,c,h}

Abstract. A recent study by Ramirez et al. (2014) demonstrated that an atmosphere with 1.3-4 bar of CO₂ and H₂O, in addition to 5-20% H₂, could have raised the mean annual and global surface temperature of early Mars above the freezing point of water. Such warm temperatures appear necessary to generate the rainfall (or snowfall) amounts required to carve the ancient martian valleys. Here, we use our best estimates for early martian outgassing rates, along with a 1-D photochemical model, to assess the conversion efficiency of CO, CH₄, and H₂S to CO₂, SO₂, and H₂. Our outgassing estimates assume that Mars was actively recycling volatiles between its crust and interior, as Earth does today. H₂ production from serpentinization and deposition of banded iron-formations is also considered. Under these assumptions, maintaining an H₂ concentration of ~1-2% by volume is achievable, but reaching 5% H₂ requires additional H₂ sources or a slowing of the hydrogen escape rate below the diffusion limit. If the early martian atmosphere was indeed H₂-rich, we might be able to see evidence of this in the rock record. The hypothesis proposed here is consistent with new data from the Curiosity Rover, which show evidence for a long-lived lake in Gale Crater near Mt. Sharp. It is also consistent with measured oxygen fugacities of martian meteorites, which show evidence for progressive mantle oxidation over time.

Corresponding author: Natasha Batalha, neb149@psu.edu

Keywords: Mars, photochemistry, climate, volcanism, Curiosity

1. Introduction

Observations of the Martian surface reveal complex valley networks that can only be explained by running water in the distant past (Irwin et al. 2008; Grott et al. 2013). Analyses of crater morphologies (Fassett & Head 2008) suggest that this water was present circa 3.8 Ga. Further support for the warm early Mars hypothesis has been provided just recently

by new data obtained by the Mars Curiosity Rover. Deposits at Gale Crater have been interpreted as being formed in a potentially habitable fluvio-lacustrine environment (Grotzinger et al., 2013), and the rover has observed stacked sediments at Mt. Sharp in Gale Crater which suggest the presence of a lake that lasted a million years or more. This implies prolonged warm conditions and a relatively Earth-like hydrologic cycle (<http://mars.jpl.nasa.gov/msl/news/whatsnew/index.cfm?FuseAction=ShowNews&NewsID=1761>). New estimates for the global equivalent early martian water reservoir have recently been calculated to be 137 m, and this may only be a lower limit (see Section 6.2) (Villanueva et al. 2015). That said, exactly how Mars was able to maintain an environment suitable for liquid water remains an open question, as modelers have been mostly unsuccessful at recreating these types of warm and wet conditions in their simulations.

^aDepartment of Astronomy and Astrophysics, Penn State University, University Park, PA 16802, USA

^bCenter for Exoplanets and Habitable Worlds, Penn State University, University Park, PA 16802, USA

^cNASA Astrobiology Institute Virtual Planetary Laboratory

^dPlanetary Environments Laboratory, NASA Goddard Space Flight Center, 8800 Greenbelt Road, Greenbelt, MD, 20771, USA

^eCarl Sagan Institute, Cornell University, Ithaca, NY 14850, USA

^fDepartment of Astronomy, Cornell University, Ithaca NY, 14850, USA

^gCenter for Radiophysics and Space Research, Cornell University, Ithaca NY, 14850, USA

^hDepartment of Geosciences, Penn State University, University Park, PA 16802, USA

Some authors have argued that sporadic impacts during the Late Heavy Bombardment may have generated steam atmospheres and that the ensuing rainfall (about 600 m total planet wide during that entire period) carved the valley networks (Segura et al. 2002; Segura et al. 2008; Segura et al. 2012). This hypothesis seems unlikely because the amount of water required to form the valley networks is higher than that by at least three orders of magnitude, according to estimates made using terrestrial hydrologic models (Hoke et al. 2011; Ramirez et al. 2014). Extending the duration of these warm, impact-induced atmospheres is theoretically possible if cirrus clouds provide strong warming (Urata & Toon 2013); however, doing so requires high fractional cloud cover almost everywhere, and so it would be nice to see this prediction verified by independent calculations. Wordsworth et al. 2013 propose transient warming episodes caused by repeated volcanic or impact episodes, but they also find that achieving the necessary erosion rates remains challenging. Kite et al. 2013 invoke the idea that liquid water was the product of seasonal warming episodes, specifically at the equator. For seasonal melting to occur, though, there still must have been a source of precipitation and the energy to power it, so this mechanism does not resolve the issue of where the water originally came from. Most recently, Halevy & Head (2014) argued that early Mars was transiently warmed by SO_2 emitted during intense episodes of volcanic activity and that daytime surface temperatures at low latitudes (and low planetary obliquity) may have been high enough to result in rainfall. Their 1-D climate model may overestimate temperatures near the subsolar point, though, as it does not include horizontal heat transport. We discuss their hypothesis further in Section 6.1.2 below.

The late Noachian-early Hesperian period ($\sim 3.8 - 3.6$ Ga) was also characterized by substantial weathering, as evidenced by the global distribution of phyllosilicates (e.g. clays). Although phyllosilicate formation requires long-term contact between igneous rocks and liquid water (Poulet et al. 2005; Carter et al. 2013), some investigators suggest that this process could occur in the subsurface (Ehlmann et al. 2009; Meunier et al. 2012). Hydrothermal systems could accomplish this, in principle; however, they require

recharging with water, and it is unclear how this could happen if the surface was cold and dry. Other authors have argued that widespread surface clay formation is suggestive of a warmer and wetter past climate (Loizeau et al. 2010; Noe Dobrea et al. 2010; Gaudin et al. 2011; Le Deit et al. 2012; Carter et al. 2013), opposing the claim that valley network formation was the product of short climatic warming episodes (Poulet et al. 2005).

An alternative to the cold Mars hypotheses is the notion that early Mars exhibited a relatively long period of warmth characterized by a dense atmosphere dominated by greenhouse gases. Early work suggested that this could be accomplished (Pollack et al. 1987) with only CO_2 and H_2O as greenhouse gases; however, these authors erred by neglecting condensation of CO_2 . Subsequent climate modelers (Kasting 1991; Tian et al. 2010; Wordsworth et al. 2010; Forget et al. 2013; Wordsworth & Pierrehumbert 2013) have been unable to warm early Mars when CO_2 condensation is included in their simulations. However, Ramirez et al. (2014) were successful in creating above-freezing temperatures when CO_2 - H_2 collision-induced absorption effects were included in their calculations. A 5% H_2 atmosphere with a ~ 3 -bar 95% CO_2 component produced 273 K surface temperatures, and models with 10-20% H_2 produced temperatures above 290 K. The dense, CO_2 -rich atmospheres required in this and other warm early Mars models have often been criticized on the grounds that they should have left extensive carbonate sediments on the surface, none of which has been observed. But the rain falling from a 3-bar CO_2 atmosphere would have had a pH of 3.7 or less (Kasting 2010, Ch. 8), which would almost certainly have dissolved any such rocks, allowing the carbonate to be redeposited on the subsurface. Carbonates have occasionally been detected at the bottoms of fresh craters (Michalski & Niles 2010) but most craters are likely filled with dust, and so it is not obvious that the carbonates should always show up in this type of observation.

While the Ramirez et al. work found a combination of greenhouse gases that could explain a warm and wet early Mars, the feasibility of that combination has not yet been demonstrated. A 5% H_2 atmosphere requires a total hydrogen outgassing rate of 8×10^{11} H_2 molecules $\text{cm}^{-2}\text{s}^{-1}$, if hydrogen escapes at

the diffusion-limited rate (see Section 2 below). Ramirez et al. made estimates of H_2 outgassing rates on early Mars that came within a factor of 2 of this value. This factor of 2, they argued, could be recovered if hydrogen escaped from early Mars at less than the diffusion-limited rate. However, the knowledge of the escape rate of H from the martian atmosphere is poorly constrained. Part of the problem is that we do not know how water-rich early Mars might have been. Data concerning the volatile content of the martian crust have been obtained from meteorite (Kurokawa et al. 2014) and in situ (Mahaffy et al., 2015) analyses, but they still leave an order of magnitude uncertainty in the global near-surface water inventory prior to 4 Ga. While a higher escape rate could be offset by a higher volcanic H_2 outgassing rate or by supplementing volcanic H_2 with other H_2 sources, this idea has not been previously explored.

In this paper, we test the plausibility of the high- H_2 hypothesis of Ramirez et al. (2014) by using a photochemical code to study whether such an atmosphere would be sustainable over geological timescales. We do this by carefully maintaining the redox balance of each simulation, looking for self-consistent atmospheres that could maintain liquid water at the planet’s surface. These simulations allow us to infer the volcanic fluxes required to maintain the high H_2 levels needed to keep early Mars warm. We also consider the potential climatic effects of species other than CO_2 , H_2O , and H_2 – specifically CO , CH_4 , SO_2 , and H_2S . Finally, we consider whether the H_2 greenhouse hypothesis might be tested using Mars rover, orbiter, and meteorite data.

2. The atmospheric and global redox budgets

All atmospheres must be in approximate redox balance over sufficiently long time scales; otherwise, their oxidation state would change during the time frame of interest. For an H_2 -rich atmosphere, ‘long’ means time scales of tens to hundreds of thousands of years (Kasting, 2013). Both an atmospheric redox budget and a global redox budget can be computed (see, e.g., Kasting & Canfield 2012; Kasting, 2013). The global redox budget is defined as the redox budget of the

combined atmosphere-ocean system. This is the budget that is considered in models of the modern Earth’s redox balance (e.g., Holland, 2002, 2009).

To balance the atmospheric redox budget, we assume that the sources of reducing power to the atmosphere are volcanic outgassing, $\phi_{out}(Red)$, and rainout/surface deposition of oxidizing species, $\phi_{rain}(Oxi)$. The sources of oxidizing power are rainout of reduced species, $\phi_{rain}(Red)$, and the escape of hydrogen to space, $\phi_{esc}(H_2)$. Given these definitions, a balanced atmospheric redox budget should obey the following relationship:

$$\phi_{out}(Red) + \phi_{rain}(Oxi) = \phi_{esc}(H_2) + \phi_{rain}(Red) \quad [1]$$

Typically, our atmospheric photochemical model balances the redox budget to about 1 part in 10^7 . The escape rate of hydrogen is given by the diffusion-limited expression (Walker, 1977)

$$\Phi_{esc}(H_2) = \frac{b_i}{H_a} \frac{f_T(H_2)}{1+f_T(H_2)} \cong \frac{b_i f_T(H_2)}{H_a} \quad [2]$$

Here, b_i is the weighted molecular diffusion coefficient, $H_a (= kT/mg)$, is the scale height (at $T \sim 160K$, $\frac{b_i}{H_a} = 1.6 \times 10^{13} \text{cm}^{-2} \text{s}^{-1}$) and $f_T(H_2)$ is the total hydrogen volume mixing ratio: $f_T(H_2) = f(H_2) + 0.5f(H) + f(H_2O) + 2f(CH_4) + \dots$, expressed in units of H_2 molecules.

Realistic models must also balance the redox budget of the combined atmosphere-ocean system. Kasting (2013) refers to this as the *global redox budget*. His expression for this budget is as follows:

$$\begin{aligned} \Phi_{out}(Red) + \Phi_{OW} + \Phi_{burial}(CaSO_4) + \Phi_{burial}(Fe_3O_4) \\ = \Phi_{esc}(H_2) + 2\Phi_{burial}(CH_2O) + 5\Phi_{burial}(FeS_2) \end{aligned} \quad [3]$$

Here, Φ_{OW} represents oxidative weathering of the continents and seafloor, and $\Phi_{burial}(i)$ is the burial rate of species i . H_2O , CO_2 , N_2 , and SO_2 are taken as redox neutral species in this formulation.

The global redox balance takes into account processes occurring at the ocean-sediment interface, e.g., burial of organic carbon and pyrite. If we assume, as a starting point, that nothing is happening at that interface, and if oxidative weathering is neglected, then the global redox budget simplifies to

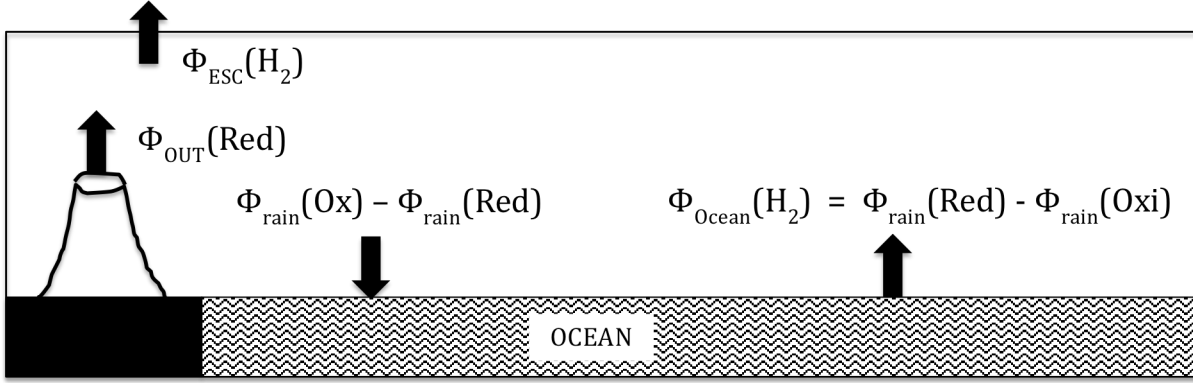


Figure 1. A schematic diagram showing the method used for balancing the ocean-atmosphere system. $\Phi_{\text{out}}(\text{Red})$ is the flux of reductants outgassed through volcanoes, $\Phi_{\text{rain}}(\text{Red/Ox})$ is the flux of rained-out reductants or oxidants (including surface deposition). $\Phi_{\text{Ocean}}(\text{H}_2)$ is the flux of H_2 back into the atmosphere required to balance the oceanic H_2 budget. An excess of reductants, such as H_2S , flowing into the ocean leads to an assumed upward flux of H_2 .

$$\phi_{\text{out}}(\text{Red}) = \phi_{\text{esc}}(\text{H}_2) \quad [4]$$

i.e., volcanic outgassing of reduced gases must be balanced by escape of hydrogen to space. Inserting this equation back into Eq. [1] implies that

$$\phi_{\text{rain}}(\text{Oxi}) = \phi_{\text{rain}}(\text{Red}). \quad [5]$$

that is, the rainout rate of oxidants from the photochemical model must equal the rainout rate of reductants. Or, to think of this in a different way, if no redox reactions are happening on the seafloor, the rate of transfer of oxidants from the atmosphere to the ocean must equal the rate of transfer of reductants. We will start from this simplifying assumption and then add seafloor processes as we proceed.

In practice, a photochemical model will *not* satisfy Eqs. [4-5] on its own. Rather, the photochemical modeler must make decisions about how to deal with any imbalance. Although previous models have typically not considered the ocean-atmosphere balance (Segura et al. 2003; Tian et al. 2010), two more recent models have done so (Domagal-Goldman et al. 2014; Tian et al. 2014). Domagal-Goldman et al. (2014) did this by wrapping the photochemical code in a separate script that repeatedly ran the model, changing the boundary conditions between simulations, until the model satisfied the above equations for a specified value of $\phi_{\text{rain}}(\text{Oxi}) - \phi_{\text{rain}}(\text{Red})$ to within a determined tolerance level.

We used the simpler procedure previously employed by Tian et al. (2014). In all of our

simulations, we found that $\phi_{\text{rain}}(\text{Oxi}) - \phi_{\text{rain}}(\text{Red})$ was < 0 , that is, the rainout rate of reductants exceeded that of oxidants. So, we let H_2 flow back from the ocean into the atmosphere at a rate equal to that of the difference between the rained out reductants and oxidants. Without this assumption, H_2 would flow back into the planet (without any physical justification), and we might therefore underestimate the atmospheric H_2 concentration. The global redox budget is illustrated in Figure 1.

By following this methodology, we essentially assume that dissolved reductants and oxidants react with each other in solution in such a way as to yield H_2 , and that the organic carbon burial rate is essentially zero. This may not always be the case, and we must be conscious of that in our analysis. For example, if the burial rate of organic carbon or other reduced species exceeded the sum of the burial rate of oxidized species and the rate of oxidative weathering, our assumptions would not apply, and atmospheric H_2 concentrations would decrease.

If all of the H_2 in the atmosphere came directly from volcanic outgassing, Eq. [2] and [4] taken together show that in order to have $f_{\text{T}}(\text{H}_2) = 0.05$, the minimum H_2 concentration needed to sustain a warm early Mars, the outgassing rate of H_2 must be at least $8 \times 10^{11} \text{ cm}^2\text{s}^{-1}$. If an appreciable fraction of the atmospheric hydrogen is in some other form, *e.g.*, CH_4 , then the total hydrogen outgassing rate would need to be correspondingly higher because the main greenhouse warming is coming from just the H_2 .

This approach allows us to consider the various sources of H_2 , including both outgassing terms and terms at the ocean-sediment interface. We outline these sources below. First, we consider contributions to $\phi_{out}(Red)$ from outgassed H_2 , S, and CH_4 . Then, we consider the contributions to $\phi_{rain}(Oxi) - \phi_{rain}(Red)$ (assumed > 0) from serpentinization and burial of iron oxides.

3. Possible sources of hydrogen on early Mars

3.1) Volcanic Outgassing

The term ‘outgassing’ refers to release of gases from magma. Volcanic outgassing rates on early Mars have frequently been estimated by looking at surface igneous rocks, evaluating their ages, and making assumptions about the volatile content of the lava from which they formed (e.g., Greeley and Schneid, 1991; Grott et al., 2011; Craddock and Greeley, 2009 and refs. therein). Grott et al. (2011) estimated that 0.25 bars of CO_2 and 5-15 m of H_2O were outgassed on Mars during the interval 3.7-4.1 Ga. The corresponding implied outgassing rates are 0.06 Tmol/yr for CO_2 and 0.3 Tmol/yr for H_2O . By comparison, the estimated outgassing rates for CO_2 and H_2O on modern Earth are 7.5 Tmol/yr and 102 Tmol/yr, respectively (Jarrard, 2003). Even taking into account the 4 times larger surface area of Earth, the implied per unit area martian outgassing rates are 25-100 times smaller. Such outgassing rates are almost certainly too small to maintain a warm, dense atmosphere, leading some to conclude that the martian atmosphere has always been thin and cold (e.g. Forget et al. 2013; Wordsworth et al., 2013; Grott et al., 2013), except, perhaps in the aftermath of repeated explosive eruptions (Wordsworth et al., 2013) or giant impacts (Segura et al., 2002).

However, these outgassing estimates for early Mars are potentially underestimated, because they ignore the effects of volatile recycling. For example, Earth’s relatively high outgassing rates result from volatile recycling between the crust and the mantle, not from juvenile degassing. Much higher outgassing rates could be expected on early Mars if the planet experienced plate tectonics and associated element recycling. Heat flow on early Mars is thought to have been comparable to that on modern Earth (Montesi & Zuber 2003), so some authors have postulated that

outgassing rates of major volatiles may also have been similar (Ramirez et al., 2014, Halevy & Head, 2014). Evidence for past tectonic activity includes Mars Global Surveyor data of an alternating polarity in the remanent magnetic field, inferred to be evidence for sea-floor spreading (Connerney 1999), and major faults associated with these crustal variations. Magnetic polarity patterns deduced by Connerney (1999) are Noachian in age, but Sleep (1994) suggests that plate tectonics extended at least through the early Hesperian. Along these same lines, Anguita et al. (2001) discuss how plate tectonics better explains the observed tectonic regime in the early Hesperian than do other hypotheses. No consensus has been reached on this topic, however; for example, Grott et al. (2013) have argued that crust-mantle recycling never occurred on Mars because plate tectonics never got started. Although the notion that plate tectonics may have operated on early Mars remains controversial, it is required to support the thick, H_2 -rich atmospheres proposed by Ramirez et al. Therefore, we assume here that Mars *did* recycle volatiles and that the overall efficiency of recycling was comparable to that on modern Earth. Future exploration of Mars will reveal whether this assumption is correct. We also consider other sources of hydrogen from oxidation of crustal ferrous iron and from photochemical oxidation of other reduced gases.

3.1.1 H_2

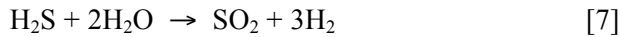
Differences in the composition of volatiles outgassed on Mars compared to Earth should result from the different oxidation states of their respective mantles. Earth’s upper mantle is thought to have an average oxygen fugacity, fO_2 , near that of the QFM (quartz-fayalite-magnetite) synthetic buffer. At typical surface outgassing conditions (1,450 K, 5 bar pressure), this yields $fO_2 \approx 10^{-8.5}$ (Frost et al. 1991; Ramirez et al. 2014). Given this value for fO_2 , the $H_2:H_2O$ ratio, R , in the gas that is released can be calculated from the expression

$$\frac{P_{H_2}}{P_{H_2O}} \equiv R = \left(\frac{K_1}{fO_2} \right)^{0.5}, \quad [6]$$

Here, P_{H_2} and P_{H_2O} are the partial pressures of the two gases, and K_1 ($=1.80 \times 10^{-12}$ atm) is the equilibrium constant for the reaction: $2H_2O \xrightleftharpoons{K_1} 2H_2 + O_2$ (Ramirez

et al., 2014). Plugging K_1 and the terrestrial mantle f_{O_2} into Eq. [6] gives an $H_2:H_2O$ ratio of 0.024. This yields a terrestrial H_2 outgassing flux of ~ 2.4 Tmol/yr, when multiplied by the terrestrial H_2O subaerial outgassing rate of 100 Tmol/yr, or $\sim 3.7 \times 10^{11} \text{ cm}^{-2}\text{s}^{-1}$ (Jarrard 2003). (On Earth, the conversion from geochemical to atmospheric science units is $1 \text{ Tmol/yr} = 3.74 \times 10^9 \text{ cm}^{-2}\text{s}^{-1}$.) The terrestrial H_2 outgassing rate is therefore of the order of $1 \times 10^{10} \text{ cm}^{-2}\text{s}^{-1}$, with a factor of 2 or more uncertainty in either direction (Holland 2009).

Mars' oxygen fugacity is thought to be at least 3 log units lower than Earth's, near $\sim IW+1$ (Grott et al. 2011). IW is the iron-wüstite buffer, which has an f_{O_2} about 4 log units below QFM. Based on this observation, Ramirez et al. (2014) calculated that Mars could have outgassed H_2 at up to 40 times the rate of Earth: $40 \times 10^{10} \text{ cm}^{-2}\text{s}^{-1} = 4 \times 10^{11} \text{ cm}^{-2}\text{s}^{-1}$. This estimate included a 50 percent contribution from H_2S , which was assumed to be oxidized to SO_2 by atmospheric photochemistry, according to



We demonstrate in the next section that this assumption may be unfounded, and so outgassing of H_2S may not have added much H_2 to Mars' atmosphere. That said, terrestrial H_2 outgassing estimates are uncertain by about a factor of 2 or more, and the early Martian mantle could have had an oxygen fugacity near IW-1 (Warren & Gregory 1996). The latter factor alone could have approximately doubled the estimated H_2 outgassing rate (Ramirez et al., 2014). Thus, an H_2 outgassing rate of $8 \times 10^{11} \text{ cm}^{-2}\text{s}^{-1}$ is not implausible; it just requires slightly more optimistic assumptions than have hitherto been adopted. Specifically, this higher outgassing rate is highly dependent on the estimate of the redox state of the ancient Martian mantle, and is the single largest source of uncertainty in our estimates of Martian H_2 outgassing rates. This highlights the importance of future measurements that might reduce the uncertainties in that quantity.

3.1.2 Sulfur

Several hundred millibar to as much as 1 bar of sulfur may have been outgassed via juvenile degassing throughout Martian history (Craddock & Greeley 2009). This leads to a sulfur outgassing rate of at most

$6 \times 10^6 \text{ cm}^{-2}\text{s}^{-1}$, if we assume it was outgassed over a period of ~ 1 billion years. As with other estimates of juvenile degassing, this small outgassing rate is not enough to maintain a warm, dense atmosphere on early Mars. On Earth, volcanic sulfur comes from three main sources: arc volcanism, hotspot volcanism, and submarine volcanism.

Direct satellite measurements of arc volcanism yield SO_2 outgassing rates of 0.2-0.3 Tmol/yr (equivalent to $\sim (0.7-1.1) \times 10^9 \text{ cm}^{-2}\text{s}^{-1}$ via the conversion above) (Halmer et al. 2002). These numbers probably underestimate the total SO_2 outgassing rate, as they only measure the SO_2 outgassed through explosive volcanism. Instead, if we combine the ratio of total sulfur to H_2O in arc volcanism (~ 0.01 in Fig 6, Holland 2002) and the ratio of H_2O to CO_2 (~ 30 in Fig 6, Holland 2002), then the rate of SO_2 outgassing on modern Earth should be ~ 0.8 Tmol/yr, assuming a CO_2 outgassing rate from arc volcanism of ~ 2.5 Tmol/yr (Jarrard 2003).

Hotspot volcanism, such as that which occurs in Hawaii, also contributes to sulfur outgassing. Although hotspot outgassing rates are difficult to accurately determine, the observed ratio of SO_2/CO_2 is ~ 0.5 (Walker 1977, Table 5.5). Therefore, if the release rate of carbon from hotspot volcanism on Earth is 2 Tmol/yr (Jarrard 2003), the corresponding release rate of SO_2 should be ~ 1 Tmol/yr. This leads to a total subaerial SO_2 outgassing rate of 1.8 Tmol/yr or $\sim 6.7 \times 10^9 \text{ cm}^{-2}\text{s}^{-1}$.

Sulfur is also outgassed as H_2S during submarine volcanism. Holland (2002) averaged measurements of H_2S concentrations in hot, axial vent fluids, 3-80 mmol/kg (Von Damm 1995; Von Damm 2000), to estimate dissolved H_2S concentrations of 7 mmol/kg. By combining this value with estimates for the total emergent water flux, $\sim 5 \times 10^{13} \text{ kg/yr}$, we can convert the H_2S concentration to an H_2S outgassing rate of 0.35 Tmol/yr, or $\sim 1.3 \times 10^9 \text{ cm}^{-2}\text{s}^{-1}$.

Gaillard & Scaillet (2009) show that on Mars, H_2S and SO_2 should be outgassed at approximately the same rate for a mantle redox state near IW. Therefore, we use an outgassing rate of $5 \times 10^9 \text{ cm}^{-2}\text{s}^{-1}$ for both SO_2 and H_2S , which is roughly in agreement with the values above. We note parenthetically that Halevy and

Head (2014) assumed that all sulfur outgassed on early Mars was in the form of SO_2 .

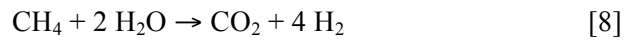
3.1.3 Carbon

On modern Earth carbon is outgassed as CO_2 at a rate of $\sim 7.5 \text{ Tmol/yr}$ ($2.8 \times 10^{10} \text{ cm}^2 \text{ s}^{-1}$) (Jarrard 2003). We expect that carbon outgassing should have also been a major contributor to the early martian atmosphere. A recent study by Wetzel et al. (2013) showed that carbon should be stored in different forms in planetary mantles, depending on the oxygen fugacity, $f\text{O}_2$. At $f\text{O}_2$ values above IW-0.55, carbon is stored as carbonate in the melt and would be outgassed as CO_2 . At $f\text{O}_2$ values below IW-0.55, carbon is stored as iron carbonyl, $\text{Fe}(\text{CO})_5$, and as CH_4 and would be outgassed as CO and CH_4 . Wetzel et al. (2013) calculated that initial solidification of a 50 km-thick crust should lead to outgassing of 1.3 bar CH_4 and 1 bar CO at low $f\text{O}_2$ or to 11.7 bar of CO_2 at higher $f\text{O}_2$. The higher pressure of the outgassed CO_2 atmosphere is caused by a factor of two increase in carbon solubility in melts at $f\text{O}_2 > \text{IW-0.55}$, along with the higher molecular weight of CO_2 compared to CO and CH_4 . Assuming this gets released over ~ 1 billion years, we derive a lower bound estimate for carbon outgassing of $6 \times 10^6 \text{ cm}^2 \text{ s}^{-1}$ at low $f\text{O}_2$ or about twice that value at higher $f\text{O}_2$. As pointed out earlier, juvenile outgassing rates are always relatively small.

A low rate of carbon outgassing may not be an issue for the CO_2 content of the early martian atmosphere because the CO_2 removal rate from silicate weathering depends on temperature. At low surface temperatures, liquid water would not be present and so CO_2 would not be lost by this process. 11.7 bar of CO_2 , or even half that amount, is more than adequate for the greenhouse atmospheres postulated here. CO_2 could also have been lost by solar wind interactions, as happens today, but such loss might have been precluded if Mars had a magnetic field at this time. We assume that the early martian atmosphere was not being rapidly stripped away in this manner.

Here, we are interested in whether outgassing of carbon in reduced form could have provided an additional source of H_2 . Outgassing rates *do* matter in this case because hydrogen is always being lost to space, regardless of the presence or absence of a magnetic field. At low mantle $f\text{O}_2$ values, outgassing

of the reduced gases CO and CH_4 could have contributed to the atmospheric H_2 budget. The outgassing rate computed from initial crustal solidification would not have been high enough to supply an appreciable amount of additional H_2 . To obtain a higher estimate, consistent with our estimate for direct H_2 outgassing above, we used modern Earth carbon outgassing estimates (Jarrard 2003) and assumed that mantle $f\text{O}_2$ was $< \text{IW-0.55}$ and that CO and CH_4 were released in the 1:1.3 ratio calculated by Wetzel et al. This yields outgassing rates of $2 \times 10^{10} \text{ cm}^2 \text{ s}^{-1}$ and $8 \times 10^9 \text{ cm}^2 \text{ s}^{-1}$ for CH_4 and CO , respectively. If all of the CH_4 was oxidized to CO_2 following the stoichiometry

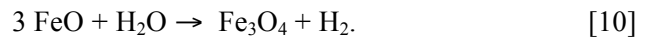


the equivalent H_2 production rate should have been 4 times the CH_4 outgassing rate, or $8 \times 10^{10} \text{ cm}^2 \text{ s}^{-1}$. This is about $1/10^{\text{th}}$ the H_2 flux needed to sustain a warm $\text{H}_2\text{-CO}_2$ greenhouse atmosphere. CO outgassing is less important as a source of H_2 , as its outgassing rate is lower and its stoichiometric coefficient for H_2 production, assuming oxidation to CO_2 , is only unity

$$\text{CO} + \text{H}_2\text{O} \rightarrow \text{CO}_2 + \text{H}_2. \quad [9]$$

3.2 Serpentinization

A second possible source of hydrogen to Mars' early atmosphere is serpentinization. This process differs from volcanic outgassing in that it occurs at relatively low temperatures, 500-600 K, whereas outgassing from magmas occurs at the melt temperature of $\sim 1450 \text{ K}$. Serpentinization occurs when warm water interacts with ultramafic (Mg- and Fe-rich) basalts. Ferrous iron contained in the basalts is excluded from the serpentine alteration products, and so it forms magnetite, releasing H_2 in the process



Evidence for serpentinization on Mars exists in the form of ultramafic rocks discovered on the Martian surface. Olivine concentrations of 10 – 20% have been detected both by the Thermal Emission Spectrometer (Koeppen & Hamilton 2008) and in SNCs (e.g. McSween et al. 2006). Moreover, the Mars Reconnaissance Orbiter (MRO) has detected serpentine itself from orbit (Ehlmann et al. 2009).

Serpentinization is a minor source of hydrogen to Earth's current atmosphere, accounting for ~ 0.4

Tmol H_2/yr , or $1.5 \times 10^9 \text{ cm}^{-2}\text{s}^{-1}$ (Sleep 2005; Kasting, 2013). For this process to have made an important contribution to the early martian H_2 budget, it would have needed to occur 10-100 times faster than it does on Earth today. That sounds daunting, but it may be possible. Most oceanic basalts today are *not* prone to serpentinization because the terrestrial seafloor is predominantly mafic, not ultramafic. Ultramafic rocks, e.g., peridotites, are found deep within the seafloor and are exposed to hydrothermal circulation within slow-spreading ridges such as the Mid-Atlantic Ridge. Earth's upper mantle should have been hotter in the past; hence, the degree of partial melting during seafloor creation should have been higher, and the seafloor itself should have been more mafic, or even ultramafic. Similarly, if Mars' upper mantle was originally hot, and if seafloor was being generated there as it is here on Earth, interaction of ultramafic rocks with water may have been commonplace, as well.

One can make a crude estimate of the H_2 flux that might have been generated by this process by drawing an analogy to seafloor oxidation on Earth today. The rate at which ferric iron is generated and carried away by seafloor spreading today is about $21 \times 10^3 \text{ kg/s}$, or $1.2 \times 10^{13} \text{ mol/yr}$ (Lécuyer & Ricard 1999). Most of this ferric iron is produced by sulfate reduction, not by serpentinization. But if the oceanic crust were more ultramafic, and if this same amount of ferric iron were generated by serpentinization, then according to reaction [10] it would produce 1 mole of H_2 for every 2 moles of ferric iron (because Fe_3O_4 contains two atoms of ferric iron), and so the corresponding H_2 flux would be 6 Tmol/yr, or $2.2 \times 10^{10} \text{ cm}^{-2}\text{s}^{-1}$. That is roughly 10% of the volcanic H_2 outgassing rate estimated by Ramirez et al. (2014) for early Mars with a mantle $f\text{O}_2$ near IW+1. So, unless martian seafloor was serpentinizing much faster than terrestrial seafloor gets oxidized today, this process would have been a relatively minor term in the martian H_2 budget. When we do the estimate this way,

serpentinization appears to be a relatively minor source of H_2 . Other authors however, have made more generous estimates of H_2 production from this process, as high as 35 Tmol/yr (on Mars), or $4 \times 10^{11} \text{ cm}^{-2}\text{s}^{-1}$ (Chassefière et al. 2014), about half the flux needed to sustain a 5% H_2 mixing ratio. So we should not rule out serpentinization as an important source of hydrogen on early Mars.

3.3 Photochemical Fe oxidation

On Earth, Fe oxidation by way of UV irradiation of surface waters could have also been a source of H_2 and could have contributed to the deposition of banded iron-formations (BIFs) (Braterman et al. 1983). Additionally, Hurowitz et al. (2010) showed that the sedimentary rocks found at Meridiani Planum on Mars were formed in the presence of acidic surface waters and that Fe oxidation may have played a role in maintaining that high acidity. This mechanism could potentially have produced large amounts of gaseous H_2 . Still, it is uncertain how much of the martian surface was producing H_2 in this manner, as Meridiani Planum has an area of $\sim 2 \times 10^5 \text{ km}^2$, only $\sim 0.1\%$ the total surface area of Mars (Hurowitz et al. 2010).

To get around this problem, we once again make an analogy to early Earth. Kasting (2013) estimated H_2 production rates from deposition of BIFs on the Archean Earth. His estimates ranged from (0.2-25) Tmol(H_2)/yr, or $(0.7-9) \times 10^{10} \text{ cm}^{-2}\text{s}^{-1}$. But the higher end of this range is an extremely generous upper bound which would require dissolved Fe^{+2} concentrations in vent fluids that were hundreds of times higher than those in modern terrestrial hydrothermal systems. Even with those assumptions, this mechanism would likely have been only a minor source of H_2 on early Mars. Despite its apparent lack of importance, we parameterize these potential effects below, because of their possible relationship to sedimentary layers on Mars, including the hematite beds on Mount Sharp in Gale Crater.

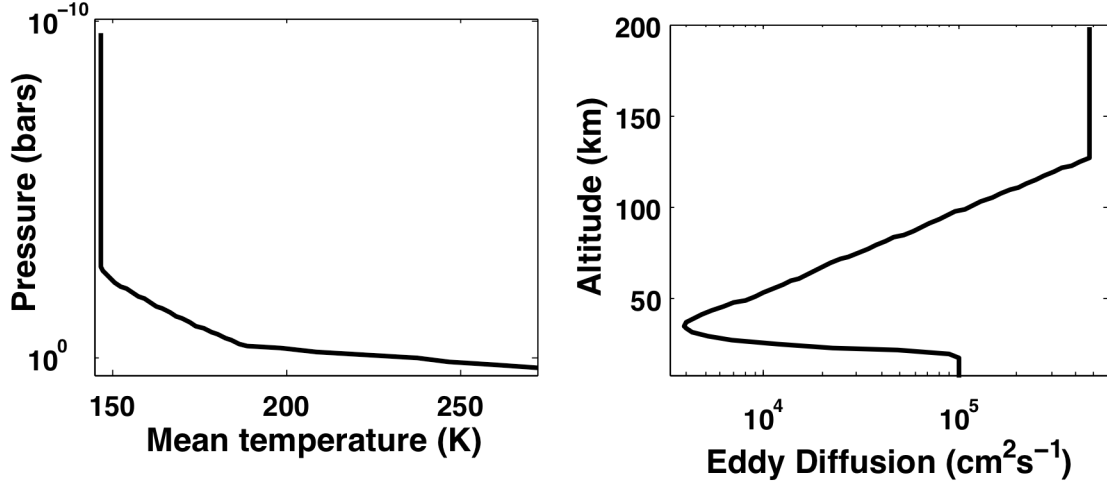


Figure 2. Temperature-pressure profile (top) and eddy diffusion profile (bottom) assumed for the photochemical calculations. The temperature decreases from 273K to 147K at an altitude of 67 km and then is isothermal to the top (200 km altitude). This is consistent with the 5% H_2 , 95% CO_2 3-bar atmosphere from Ramirez et al. 2014.

4. Model Description

4.1 Photochemical Model

To investigate how fast volcanic gases such as H_2S and CH_4 would be converted into H_2 , we used a 1-D (in altitude), horizontally averaged photochemical model that solves the coupled continuity and flux equations for multiple atmospheric species using an implicit, reverse Euler integration technique. The model, originally developed by (Kasting et al. 1979), has been most recently updated by (Domagal-Goldman et al. 2011). The model used for this study does not include higher hydrocarbon chemistry (alkenes, alkynes, alkanes longer than C_2), as it is not important for the current calculation. Instead, the model includes 29 long-lived species and 16 short-lived species involved in 215 reactions (see Appendix A).

The model consists of 100 plane parallel layers spaced by 2 km in altitude, allowing it to calculate species profiles up to 200 km. We begin by assuming that Mars was wet and warm with a surface temperature of 273 K. These parameters were chosen to be consistent with a temperature-pressure profile derived by Ramirez et al. 2014 for a 3-bar, 5% H_2 , 95% CO_2 atmosphere. This assumed composition ignores the possible presence of higher amounts of N_2 in the early martian atmosphere, which can be inferred

from the high measured $^{15}\text{N}/^{14}\text{N}$ ratio today (Fox 1993). Higher N_2 should not greatly affect the climate; indeed, N_2 can substitute for CO_2 to create pressure-induced absorption by H_2 (Ramirez et al., 2014, Fig. 2). Whether our assumed composition is an accurate representation of the early martian atmosphere depends, of course, on the validity of the Ramirez et al. hypothesis. However, the point of this study is to see if such an atmosphere is sustainable, so the use of it here is consistent with that goal. This means atmospheres that do not reproduce the Ramirez et al. H_2 concentrations have an inconsistent temperature profile; however any simulations that could maintain such an atmosphere would be self-consistent. The temperature is assumed to decrease from 273 K at the surface to 147 K at an altitude of 67 km, following a moist H_2O adiabat in the lower troposphere (0-20 km) and a moist CO_2 adiabat above that (20-120 km). Above 67 km, the atmosphere is assumed to be isothermal up to 200 km altitude, consistent with the assumed lack of oxygen and ozone. Several reactions rates are positively correlated with temperature (i.e. an increase in temperature causes an increase in the rate of a reaction). In the case of water vapor, a 10 K increase in temperature doubles the water vapor volume-mixing ratio. H_2 , however, is less affected (1% increase) by this same change in temperature. Figure 2

shows this temperature profile along with the eddy diffusion profile.

3.2 Boundary Conditions

At the top of the atmosphere, CH₄, H and H₂ are assumed to diffuse upward at the diffusion-limited velocity (Walker 1977), while CO and O are given constant downward fluxes that balance photolysis of

Table 1. Deposition Velocities at Lower Boundary

Species	Deposition Velocity (cm/s)
O	1
O ₂	0
H ₂ O	0
H	1
OH	1
HO ₂	1
H ₂ O ₂	0.2
CO	1×10^{-8}
HCO	1
H ₂ CO	0.1
CH ₄	0
CH ₃	1
C ₂ H ₆	1×10^{-5}
NO	3×10^{-4}
NO ₂	3×10^{-3}
HNO	1
H ₂ S	0.015
HS	3×10^{-3}
S	1
HSO	1
SO	3×10^{-4}
SO ₂	1
NH ₃	0
NH ₂	0
N	0
N ₂ H ₄	0
N ₂ H ₃	0
H ₂ SO ₄	0.2

CO₂ above the top layer of our model. All other species are assigned a flux of zero at the top of the atmosphere, implying that nothing else is escaping besides hydrogen. This assumption is consistent with the presence of a magnetic field to prevent solar wind stripping and with hydrodynamic escape rates for heavy species that were slower than those calculated by (Tian et al. 2009)(whose escape model did not include appreciable concentrations of H₂).

At the lower boundary, every species except for H₂ was given a constant deposition velocity. (As stated in Section 2, H₂ was assigned a constant upward flux at the lower boundary to ensure redox balance.) This accounts for their reaction with surface rocks and any ocean that might have been present. Table 1 lists the assumed deposition velocities for each species. Our results are insensitive to most of these deposition velocities, with the notable exception of CO. In most of our simulations, the CO deposition velocity is fixed at 10^{-8} cm s⁻¹, the value derived for an abiotic early Earth (Kharecha et al. 2005). The assumption here is that dissolved CO equilibrates with formate, but that a small percentage of that formate is photochemically converted to acetate and is lost from the atmosphere-ocean system. This implies that there is a small, but finite, burial flux of organic carbon (as acetate). Sensitivity tests, described below, were performed to determine the effect of varying the CO deposition velocity.

4.3 Volcanic Outgassing

Six different gases, H₂, CO, CH₄, NH₃, SO₂, and H₂S, were assumed to have sources from volcanic outgassing. CO₂ has a volcanic source, as well, but the CO₂ mixing ratio is fixed in our model at 0.95. The other 5% of the atmosphere is assumed to consist of N₂. When H₂ builds up to appreciable concentrations in the model, it displaces CO₂. Volcanic fluxes for the base case and final model are listed in Table 2. These fluxes were distributed over the lowest 20 km of the troposphere, leaving the bottom boundary of the model free to simulate atmosphere-ocean exchange.

5. Photochemical Results

The photochemical profiles of major constituents, sulfur species, nitrogen species and hydrocarbon species in the base case model are shown in Figure 3.

The base case was modeled with the outgassing rates shown in Table 2. With these relatively low rates the base case was dominated by CO_2 (95%) and N_2 (5%). H_2 and CO were both in the 0.1% range, while CH_4 and H_2S were trace gases at 0.3 ppmv and 0.1 ppbv, respectively.

Next, we increased H_2 , sulfur ($\text{SO}_2/\text{H}_2\text{S}$), and carbon (CO/CH_4) outgassing to test whether or not the reducing species would effectively convert to H_2 . Figure 4 shows the effect of increasing H_2 outgassing on the H_2 mixing ratio. As one would expect based on Eqs. [2] and [4], this produced a linear relationship. But figure 4 also shows the possible increase in atmospheric H_2 from the H_2 sources discussed in Section 3, namely, ferrous iron oxidation and serpentinization. In order to get up to 5% H_2 by this

mechanism, the net H_2 sources would need to be ~ 80 times larger than the modern terrestrial H_2 outgassing rate. We can get about half of this hydrogen from direct volcanic outgassing of H_2 if the mantle $f\text{O}_2$ was near IW-1. Serpentinization is also a significant H_2 source (see Table 3). BIF deposition could contribute smaller amounts of H_2 . If serpentinization was not as efficient as assumed here, then either volcanic outgassing rates must have been higher than we have assumed, or hydrogen escape must have been slower in order to reach the required 5% atmospheric H_2 .

We then returned to a negligible H_2 outgassing rate and varied only the sulfur outgassing, keeping SO_2 and H_2S outgassing rate in a 1:1 ratio. If the H_2S is directly converted to H_2 we would also expect a linear relationship between the outgassing rate and $f(\text{H}_2)$.

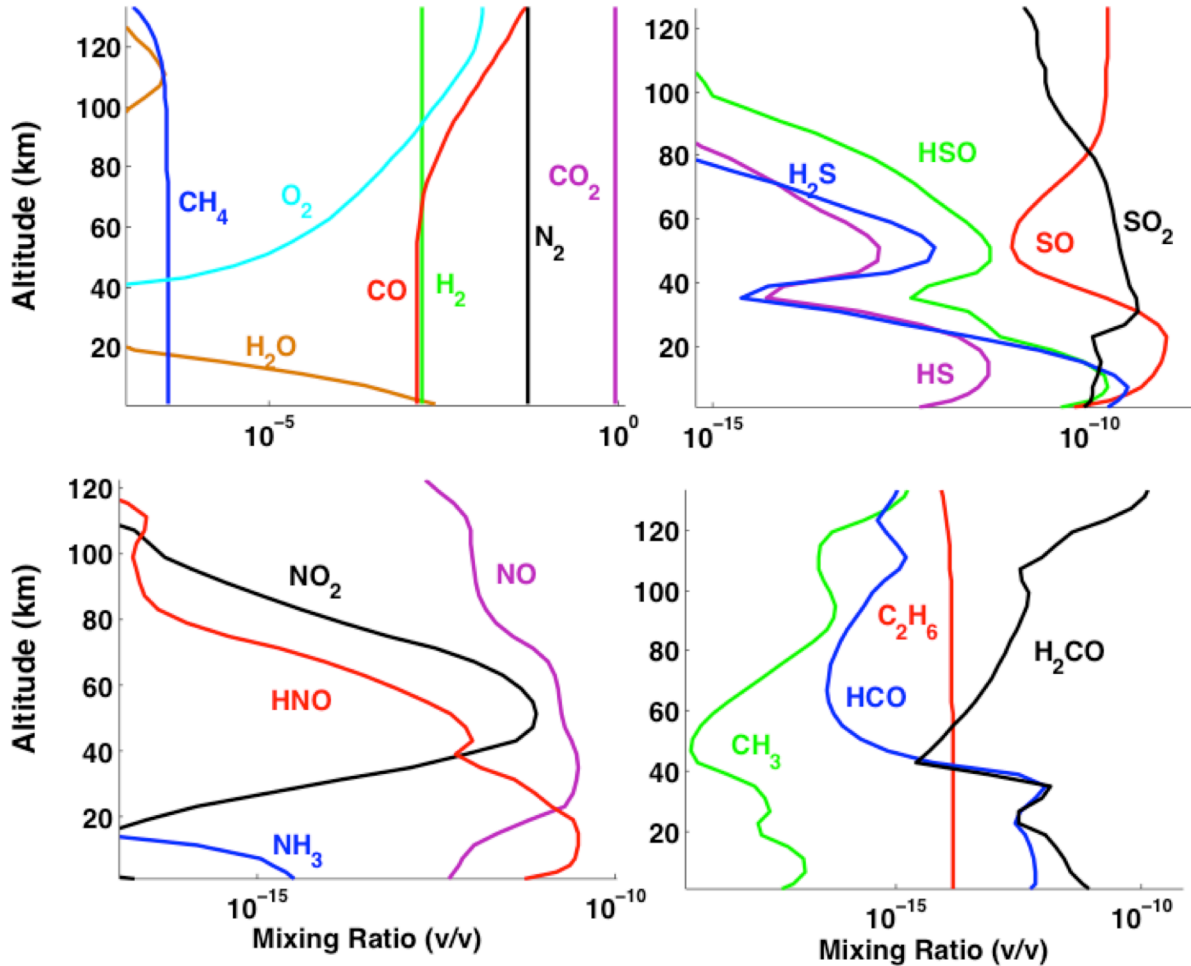
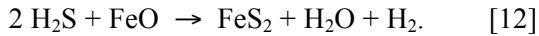


Figure 3. Mixing ratios of different species in the base case martian atmosphere assuming the (minimal) outgassing rates from Table 2. Major constituents are shown in the top left, sulfur species in the top right, nitrogen species in the bottom left, and less abundant hydrocarbons in the lower right.

Table 2. Total outgassing values

Outgassing Rate (cm^2s^{-1})	H_2	SO_2	H_2S	CH_4	CO	NH_3
Base Case	1×10^{10}	5.4×10^9	5.4×10^9	5×10^6	0.0	1.7×10^5
5% H_2 Case	8×10^{11}	5.4×10^9	5.4×10^9	1.9×10^{10}	8×10^9	1.7×10^5

Instead, we found that this relationship depended on what chemistry was assumed to be occurring in the ocean. If H_2S was converted to H_2 and SO_2 in solution, then the stoichiometry is given by Eq. [7], and our models produce the linear relationship shown by the blue solid curve in Figure 5. By analogy with early Earth, however, it seems more likely that H_2S would have reacted with dissolved ferrous iron to form pyrite, FeS_2 . The redox reaction in this case can be written as



Based on this stoichiometry, 0.5 mole of H_2 should be generated for each mole of H_2S outgassed. This yields the blue dashed curve in Figure 5, which has a more gradual rise in the H_2 mixing ratio, as compared to the

solid curve ($\sim 1/6^{\text{th}}$ the solid line). We conclude that H_2S outgassing was at best a minor source of atmospheric H_2 .

Additionally, we find that at terrestrial SO_2 outgassing rates ($5.4 \times 10^9 \text{ cm}^2\text{s}^{-1}$), H_2S becomes the dominant sulfur species: its concentration was ~ 0.1 ppbv (solid curve in figure 5), while SO_2 was a factor of 2-3 lower. Halevy and Head (2014) argue that Mars could have rapidly outgassed SO_2 over brief intervals at rates that were a few thousand times higher than modern Earth ($\sim 10^{12} \text{ cm}^2\text{s}^{-1}$), leading to 10 ppmv SO_2 . If SO_2 outgassing rates were at those levels, then so were the rates of H_2S , and the early martian atmosphere would have been even more highly

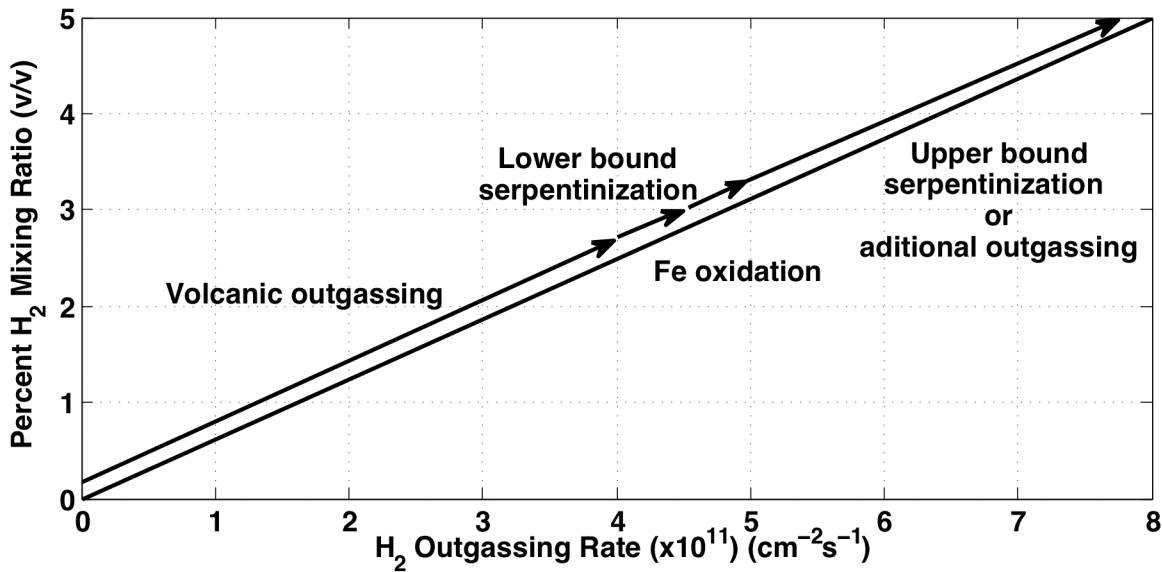


Figure 4. Calculation showing the effect of H_2 outgassing rate on H_2 mixing ratio, along with the different sources of H_2 thought to contribute to the overall outgassing rate. The escape rate is assumed to be diffusion-limited, as discussed in the text.

reducing.

We repeated this process for carbon outgassing, with the results shown in figure 6. On early Mars, carbon would have been outgassed as a combination of CH_4 and CO , in the ratios discussed in Section 3.1.3. As with sulfur, it is theoretically possible that some of this outgassed carbon could have been deposited in reduced form in sediments. (This is represented by the term $\Phi_{\text{burial}}(\text{CH}_2\text{O})$ in eq. [3].) But formation of organic carbon on Earth is almost entirely biological; thus, for an abiotic early Mars, this term would probably have been small. It seems more likely that both CH_4 and CO were converted to CO_2 and H_2 , following the stoichiometry of eqs. [8] and [9]. Therefore, carbon outgassing could have made a significant contribution to the H_2 concentration in the early Martian atmosphere, raising it to as high as 0.4%. But it would not have pushed the H_2 mixing ratio above 5% unless total carbon outgassing rates on early Mars were substantially higher than those on modern Earth.

When the carbon outgassing rate was high, the CO volume mixing ratio reached 9%, and the model atmosphere entered a regime referred to as “ CO runaway” (Zahnle 1986; Kasting et al. 1983). The primary sink for CO in this situation is the flux of CO into the ocean. Because little is understood about the rate at which CO will decompose in solution, it is difficult to accurately constrain the CO deposition

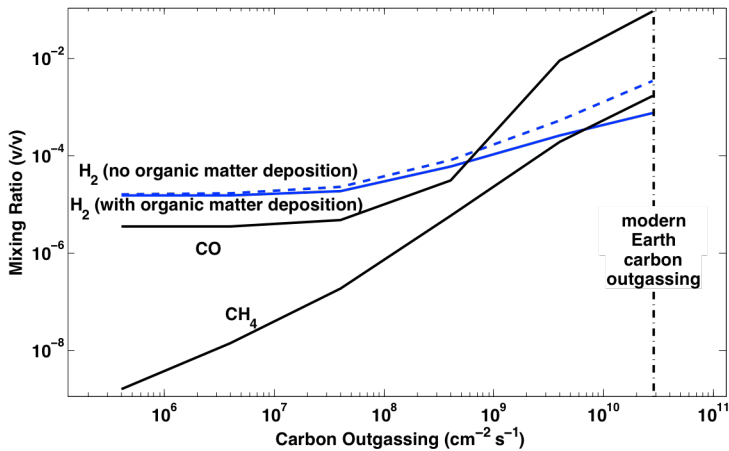


Figure 6. Calculation showing the effect of carbon outgassing rate on the atmospheric H_2 mixing ratio. At total carbon outgassing rates $> 3 \times 10^{10} \text{ cm}^{-2} \text{ s}^{-1}$, the atmosphere goes into CO runaway (see discussion in text).

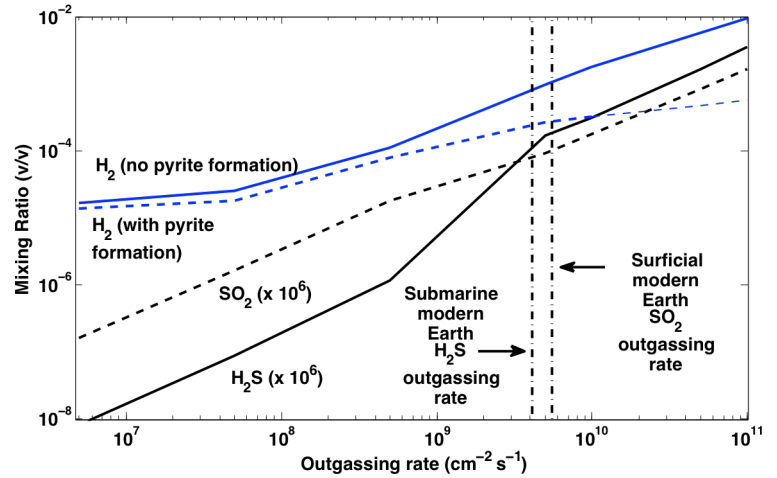


Figure 5. Calculation showing the effect of sulfur ($\text{SO}_2/\text{H}_2\text{S}$) outgassing rate on the atmospheric H_2 mixing ratio. The blue dashed curve is the H_2 mixing ratio under the assumption that H_2S reacts to form pyrite, as seems likely. The blue solid curve shows what happens if all of the H_2S dissolved in the ocean returns back to the atmosphere as a flux of H_2 (less likely).

velocity. As a result, different authors employ different values. Kharecha et al. (2005) derived an abiotic CO deposition velocity of 10^{-9} - $10^{-8} \text{ cm s}^{-1}$, based the assumption that dissolved CO equilibrates with formate, but that a small percentage of the formate is photochemically converted to acetate and is lost from the atmosphere-ocean system. If CO -consuming bacteria were present in the ocean, holding the dissolved CO concentration near zero, the CO deposition velocity would have been much higher, $\sim 1.2 \times 10^{-4} \text{ cm s}^{-1}$. Tian et al. (2014) simply logarithmically averaged these biotic and abiotic deposition velocities. There is no obvious physical justification for this assumption. Figure 7 shows a linear correlation between CO deposition velocity and CO volume mixing ratio. The loose constraint on this lower boundary condition makes it difficult to rule out the possibility of a CO -dominated atmosphere. In the limiting case where the deposition into the surface is not a sink for CO (CO deposition velocity = 0), the model atmosphere contains $\sim 50\%$ CO by volume. More work on the behavior of CO in solution is needed to constrain these possibilities.

Table 3. H_2 Sources and Respective Yields

H_2 Source	H_2 yield lower limit [$\times 10^{10} \text{ cm}^{-2} \text{ s}^{-1}$]	H_2 yield upper limit [$\times 10^{10} \text{ cm}^{-2} \text{ s}^{-1}$]	Value in 5% H_2 model [$\times 10^{10} \text{ cm}^{-2} \text{ s}^{-1}$]
H_2	20	40	40
S ($\text{SO}_2 + \text{H}_2\text{S}$)	0.25	3.0	0.25
CH_4	0.0012	8	8
Serpentinization	0.15	40	20
Fe-oxide burial	0.7	9	9
Total	21	100	77

Finally, figure 8 shows profiles of major atmospheric species after adding volcanic outgassing in the amounts shown in the Table 2. Table 3 shows a breakdown of the outgassing sources contributing to 5% H_2 compared to their upper and lower limits. In order to determine what would be required to maintain the H_2 greenhouse proposed by Ramirez et al. (2014), we simply assumed that the various outgassed fluxes add up to the required value. For this atmosphere, CO constituted $\sim 9\%$ (by volume) of this atmosphere, and the CH_4 mixing ratio was just under 2000 ppmv. Surprisingly, this large amount of CH_4 has little effect on the climate (see discussion below). Based on the discussion above, all but a small fraction of the H_2 in

this atmosphere must have come from direct H_2 sources, such as H_2 outgassing, ferrous iron oxidation, and serpentinization.

6. Discussion

6.1 Greenhouse warming by gases other than CO_2 and H_2

6.1.1 CO & CH_4

A 3-bar, CO_2 -dominated atmosphere with 5% H_2 could have warmed the early Martian surface. But our high-outgassing atmosphere also contained almost 2000 ppmv of CH_4 , which is considered to be a strong greenhouse gas, along with $\sim 10\%$ CO. CO has an absorption band in the $5\mu\text{m}$ region, far into the Wien tail of a blackbody with an effective temperature 235 K. Therefore, despite its high concentration, the effect of CO on climate is limited to pressure-broadening of gaseous absorption by other species and Rayleigh scattering of incident solar radiation. (We tested this just to make sure by deriving k -coefficients for CO and including it in our climate model. The effect was negligible.)

Methane's effect on climate in a dense, CO_2 -dominated martian paleoatmosphere has previously been explored (Ramirez et al. 2014; Byrne & Goldblatt 2014). Both groups find little to no warming from CH_4 . Methane has a strong absorption band at $7.7\mu\text{m}$ that is important in warming Earth's climate. However, near-infrared absorption of incoming solar radiation by CH_4 in the upper atmosphere produces stratospheric inversions that counteract this

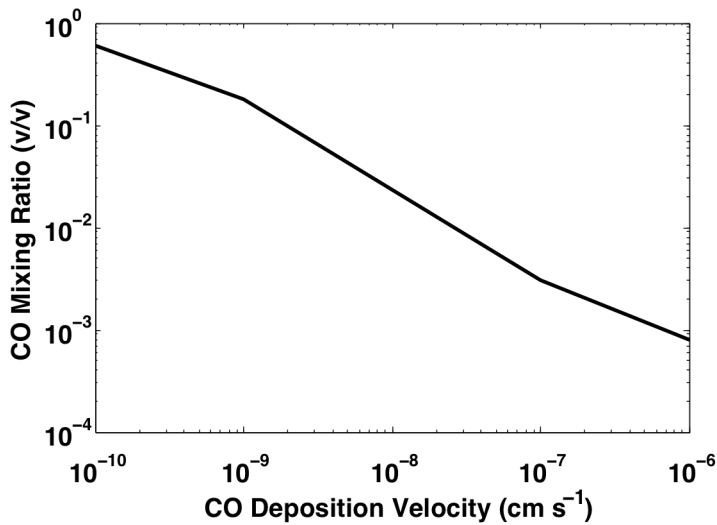


Figure 7. CO volume mixing ratio as a function of assumed deposition velocity. The atmospheric profile in Figure 8 was used for all calculations. The loose constraint on deposition velocity prevents us from determining precise values for CO

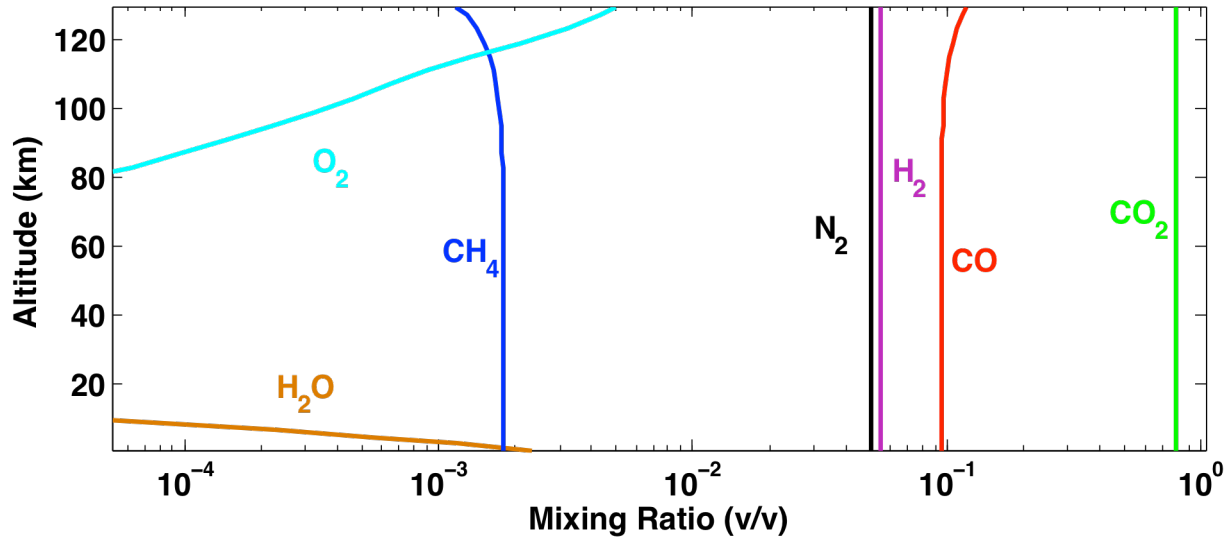


Figure 8. 1-D photochemical model results showing volume mixing ratio as a function of altitude. This is the base case early Martian atmosphere (Figure 2) after adding volcanic outgassing and balancing the redox budget for the combined ocean-atmosphere system. Here we are optimistic, and add in enough H₂ outgassing to attain a 5% H₂ atmosphere.

greenhouse warming. This stratospheric warming is particularly pronounced when new CH₄ absorption coefficients derived from the HITRAN2012 database are used (Byrne & Goldblatt 2014). Collision-induced absorption (CIA) from N₂-CH₄ interactions is significant in the 200-400 cm⁻¹ region. However, because the strong water vapor pure rotation band also absorbs in that same region (200-400 cm⁻¹), the warm atmosphere would be opaque at those wavelengths and CIA does little to help sustain this (Buser et al. 2004; Ramirez et. al. 2014). As a result, the additional warming produced by CH₄ in this atmospheres modeled here should be negligible. An important caveat is our explicit assumption that CO₂ broadening of CH₄ is no more efficient than broadening by N₂. Although experimental data for CO₂-CH₄ CIA interactions are currently unavailable, we should not rule out methane as a potential source of warming if it is later found that CO₂ is a better foreign broadening agent than N₂.

6.1.2 SO₂

As mentioned earlier, Halevy and Head (2014) suggested that warm periods lasting 10-100 years could have been produced by short, episodic bursts of SO₂. Specifically, they assumed long-term globally averaged SO₂ outgassing rates on the order of 10¹⁰ cm⁻²s⁻¹, with outgassing events on the order of 10¹² cm⁻²s⁻¹

every 1,000-10,000 years. This leads to SO₂ concentrations ranging from 0.5-2 ppmv in their model. By comparison, our assumed SO₂ outgassing rate for both the base-case and high-H₂ models is 5.4×10⁹ cm⁻²s⁻¹ (Table 2), or just over half that of Halevy and Head (2014), but our calculated SO₂ concentrations are ~3 orders of magnitude smaller. The difference is caused by our assumption that early Mars was wet and warm and that an ocean—or at least several large seas—was present at its surface. Both rainout and surface deposition are therefore important loss processes in our model, whereas the (much longer) lifetime of SO₂ in the Halevy and Head model is set by its rate of photochemical oxidation to H₂SO₄. Their model would predict smaller, shorter-lived temperature increases if rainout and surface deposition of SO₂ were included.

We note that sporadic, high-volume input of SO₂, as suggested by Halevy and Head, should have been accompanied by high-volume input of H₂. This should not have had a great impact on the atmospheric H₂ concentration, however, because the lifetime of H₂ in one of our high-H₂ atmospheres is close to half a million years. (This can be readily calculated by dividing the column mixing ratio of H₂ by the diffusion-limited escape rate given by eq. [2].) In the Halevy and Head model, slow outgassing during the long periods of relative quiescence dominates the total

volatile input, and the same should be true of H₂. 100 years of H₂ outgassing at 100 times the normal rate would have increased atmospheric H₂ concentrations by only a few percent. So, a spiky volcanic outgassing history for early Mars would not alter our hypothesis to any great extent.

6.2 S-MIF Signal Implications

A concern with the proposed H₂-dominated atmosphere is that it would have eliminated the oxidized sulfur exit channels, and thereby have precluded any sulfur mass independent fractionation (MIF) from being recorded in the rock record. This signal can be measured as $\Delta^{33}\text{S}$, the deviation of the $^{33}\text{S}/^{32}\text{S}$ ratio from the fractionation line defined by ^{34}S and ^{32}S . A recent analysis of 40 Martian meteorites reveals sulfur isotopes indicative of mass-independent fractionation (MIF) in a variety of protolithic ages - ALH 84001, the nakhlites, Chassigny and six shergottites (Franz et al. 2014). The only way to preserve such a S-MIF signal is if sulfur is distributed amongst two or more different species as they rain out of the atmosphere (Pavlov & Kasting 2002). Our simulations predict sulfur would have exited the atmosphere in at least three different exit channels, HSO, SO₂, H₂S (see Figure 9) even with 5% H₂. This suggests that an atmosphere containing 5% H₂ could still produce and record a measureable S-MIF signal.

6.3 D/H ratios, hydrogen escape rates, and initial water inventories

The recent paper by Villanueva et al. (2015) provides additional support for the idea that early Mars was warm and wet. These authors looked at deuterium/hydrogen (D/H) ratios in various water vapor masses across the martian surface and estimated an average enrichment of ~ 8 for their source regions (martian ice) relative to terrestrial seawater. When combined with an estimated modern H₂O inventory of 21 m GEL (global equivalent layer) in the polar layered deposits, an estimated initial D/H enrichment of 1.275 relative to seawater, and an assumed fractionation factor, $f = 0.02$, for escape of D relative to H, this yields a global equivalent water layer of 137 m for early Mars. The relevant mathematical relation is

$$\frac{M_p}{M_c} = \left(\frac{I_p}{I_c}\right)^{1/(1-f)} \quad [13]$$

Here, M_p and M_c are the ancient and current water reservoir sizes, respectively and I_p and I_c are the ancient and current D/H ratios.

137 m of water may sound like a lot, but in reality it is just a lower bound because the assumed fractionation factor, from Krasnopolsky et al. 1998, is only appropriate for the modern (highly tenuous) martian upper atmosphere in which nonthermal hydrogen escape processes predominate. If the early martian atmosphere was rich in H₂, as postulated here, hydrogen escape would have been hydrodynamic, and D would have been dragged off along with H, thereby increasing the fractionation factor, f . We can estimate f if we assume that H₂ was escaping at the rate of $8 \times 10^{11} \text{ cm}^{-2}\text{s}^{-1}$ required to maintain a 5% H₂ atmosphere. We assume here that hydrodynamic escape was efficient enough to keep up with the diffusion limit. The fractionation factor for hydrodynamic escape is given by (Hunten et al. 1987, eq. 17)

$$f \equiv \frac{F_2 / X_2}{F_1 / X_1} = \frac{m_c - m_2}{m_c - m_1} \quad (14)$$

Our notation is slightly different from Hunten et al., and our fractionation factor, f , is related to their factor,

y , by $f = \frac{1}{1+y}$. (The ‘ y ’ notation is convenient for

isotopes of heavy elements that differ in mass by only a small percentage, whereas the f notation is preferred for isotopes of light elements like hydrogen that have large mass differences.) Here, F_1 , X_1 , and m_1 are the escape rate, mixing ratio, and molecular mass of the lighter species (H₂), F_2 , X_2 , and m_2 are the equivalent quantities for the heavier species (HD), and m_c is the crossover mass, given by (Hunten et al., 1987, eq. 16)

$$m_c = m_1 + \frac{kTF_1}{bgX_1} \quad [15]$$

Here, k is Boltzmann’s constant, T is temperature, X_1 is the mole fraction of H₂ (≈ 1), g ($= 373 \text{ cm s}^{-2}$) is gravity, and b ($= 1.76 \times 10^{19} \text{ cm}^{-1}\text{s}^{-1}$) is the diffusion constant between H₂ and HD (Banks and Kockarts, 1973, v. 2, eq. (15.29)). We can simplify this expression by dividing through by the mass of a hydrogen atom, m_H ,

and letting $H_H = \frac{kT}{m_H g}$ be the scale height of atomic

hydrogen. Then, in atomic mass units, eq. (15) becomes

$$M_c = M_1 + \frac{F_1}{b/H_H} \quad (16)$$

If we take $T = 160$ K, then $H_H \approx 3.5 \times 10^7$ cm and $b/H_H \approx 5 \times 10^{11}$ cm²s⁻¹. For $F_1 = 8 \times 10^{11}$ cm²s⁻¹, we get $M_c \approx 3.6$ amu, and from eq. (14), $f \approx 0.4$. Then, if we take the other parameters to be the same as those assumed by Villanueva et al. (2015), Eq. (13) yields an initial water inventory of ~ 450 m, or over three times their published estimate. Higher hydrogen escape fluxes would increase this value even further, following the nonlinear relationships expressed by eqs. (13-16). We conclude that high measured D/H ratios on present Mars are consistent with a relatively deep global ocean and an H₂-rich atmosphere on early Mars. They do not require it, however, as these same high D/H ratios can be produced by loss of lesser amounts of water by mechanisms involving lower fractionation factors.

6.4 Tests for higher H₂ outgassing rates

As discussed above, a 5% H₂ atmosphere is possible if H₂ outgassing rates on ancient Mars were 8×10^{11} H₂ molecules cm⁻²s⁻¹; however, the assumed outgassing rates in our standard simulations only provide $\sim 5 \times 10^{11}$ H₂ molecules cm⁻²s⁻¹, if serpentinization did not generate significant H₂. If Mars' early atmosphere was

hydrogen-rich, at least one of our estimated H₂ outgassing sources must be too low, or else H₂ must have escaped at less than the diffusion-limited rate. The escape rate can, in principle, be investigated by constructing sophisticated theoretical models of hydrodynamic escape. This remains as work to be done. Some empirical tests of hydrogen outgassing and escape rates may be possible, either using rover measurements or by analyses of samples returned from the Martian surface. For example, Curiosity has already made a significant impact on D/H ratio measurements. D/H was measured in a ~ 3 -billion-year-old (Farley et al., 2014) mudstone at 3.0 times the ratio in standard mean ocean water (Mahaffy et al. 2015). This value is half the D/H ratio of present Mars' atmosphere, which is consistent with continued escape of hydrogen throughout Mars' history. By making similar measurements as Curiosity moves up-section in Gale Crater, and comparing these measurements to existing measurements of Martian meteorites, a history of martian D/H ratios can be constructed, and from this some information regarding the H escape rate can be inferred. Of course, getting detailed information is complicated because the fractionation between D and H during escape depends on both the rate and mechanism of the escape process. More robust tests are outlined briefly below.

6.4.1 Analyses of ancient Martian mantle redox state

The single greatest source of uncertainty in our H₂ outgassing budgets is our knowledge of the redox state of the ancient martian mantle. The majority of martian meteorites have a mantle oxygen fugacity near IW+1. But if even part of the story we have outlined here is true, then the redox state of the martian mantle must have evolved with time as H₂O was subducted and hydrogen was outgassed as H₂, leaving oxygen behind. Other authors, too, have postulated that the redox state of the martian mantle evolved over time (Richter et al. 2008). An initial redox state of IW-1, or lower, is consistent with a more reducing composition during core formation and with the low measured fO_2 of ALH 84001 (Warren & Gregory 1996; Steele et al., 2012). The fO_2 for ALH 84001 is closer to IW-1, a value that would provide a half the H₂ flux needed to maintain a 5% H₂ atmosphere, given Earth-like outgassing rates. So,

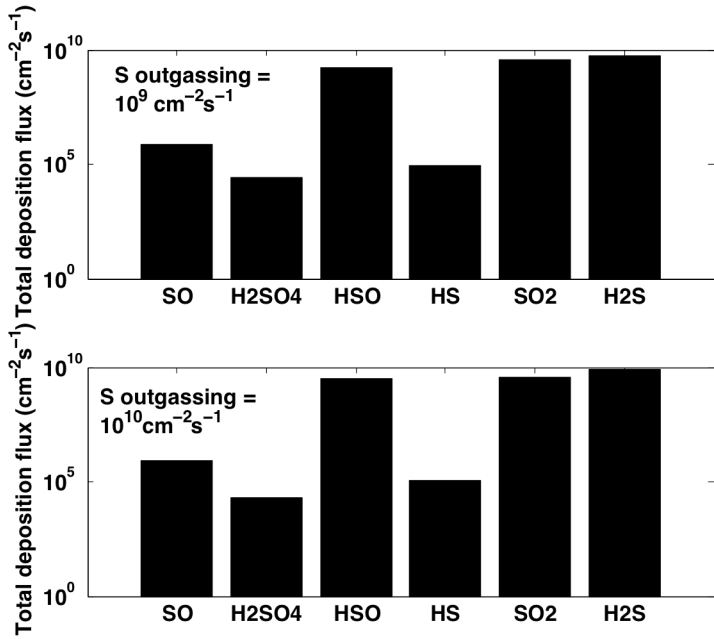


Figure 9. Total removal rate (rainout + surface deposition) for low (top) and high (bottom) cases of sulfur outgassing in an early Martian atmosphere. This shows three quantitatively important pathways that should allow for the preservation of a sulfur isotope MIF signal.

even at this point, our model requires twice Earth outgassing rates (or slower H_2 escape). As the mantle $f\text{O}_2$ increased, even higher outgassing rates would have been needed to maintain 5% H_2 . Thus, the end of the warm wet period could have been brought about either by declining outgassing rates or by progressive mantle oxidation.

Such an evolution of mantle redox state would be broadly consistent with other assumptions in our conceptual model. Deposition of oxidized iron in BIFs and subsequent subduction of these sediments would have deposited additional O in the mantle. We should note that a similar process of progressive mantle oxidation has been suggested for early Earth (Kasting 1993) but has since been largely ruled out. On Earth, these processes evidently did *not* result in a secular change in mantle redox state, presumably because Earth's mantle was already oxidized up to near the QFM buffer during or shortly after accretion (Wade & Wood 2005; Frost & McCammon 2008). The proposed oxidation process involves disproportionation of ferrous iron at high pressures in Earth's lower mantle—a process that might not have occurred on a smaller planet. If the martian mantle started out with an $f\text{O}_2$ near IW, then small additions of oxygen could conceivably have oxidized it more significantly over time. Indeed, the observed spread in $f\text{O}_2$ values of martian meteorites up to values approaching QFM suggests that mantle oxidation did occur (Stanley et al. 2011). We take this as indirect support for our hypothesis.

That said, the existing data do not allow us to draw firm conclusions about the early redox evolution of the martian mantle. The only measurement of redox state during this early phase of the planet's history comes from analyses of ALH 84001. Given the large spread in measured $f\text{O}_2$ values of younger materials, this leaves great uncertainties in the redox state at that time. Ideally, one would like to have a suite of redox measurements at multiple points in martian history, to account for the spread in the data and to constrain the temporal evolution. This is not feasible in the near future, but could happen over the coming decades with an extensive sample return campaign.

In the meantime, contextual information on this period of martian history could be obtained from Curiosity, ExoMars, and the Mars 2020 lander. Such

contextual information on the early surface evolution of Mars is one of the main goals of the Curiosity mission. Curiosity has already dated sedimentary rocks on the martian surface (Farley et al. 2014), placing an age on the deposition of the lacustrine sediments in Gale Crater (Grotzinger et al. 2013). Making subsequent time-stamped measurements would help place the rest of the results from Curiosity in an absolute historical context that could be compared to future mantle redox measurements.

This context would be augmented by qualitative estimates of the redox state of mantle-derived materials. These can be made through this measurement of the relative abundances of redox-sensitive trace elements such as Fe, for example with MSL's ChemCam. Similar instrumentation was present on the MER rovers, and planned for future rovers, so it may be possible to stitch together this history, albeit without the quantitative dating capabilities of Curiosity.

6.4.2 Analyses of Fe-oxide rich sedimentary rocks

Contextual information on the co-evolution of the Martian atmosphere and mantle may also come through analyses of ancient Fe-oxide rich layers. Although we do not expect a huge H_2 outgassing contribution from Fe-oxide deposition (see sections 3.2-3.3), the presence of Fe-oxide rich sedimentary layers is consistent with an H_2 -rich atmosphere. Such layers have an analog in the banded iron-formations (BIFs) on ancient Earth. These are thought to have required an anoxic deep ocean so that ferrous iron could be transported over long distances to upwelling regions where the BIFs formed (Holland 1973). Therefore, charting and dating the presence/absence of such layers could provide critical information on the long-term evolution of the redox state of the surface, just as the presence/absence of BIF's has had a huge impact on our assessment of the redox history of Earth's surface (Holland & Trendall 1985).

By measuring the deposition rates of the Fe-oxides, it would also be possible to estimate the H_2 outgassing rate they could have provided, both locally and, by extrapolation, globally. The Fe concentration of the samples can be measured, and the deposition times can in theory be calculated by dating the sedimentary layers on Mars (Farley et al., 2014).

However, the uncertainties of the dating measurements (± 0.35 Ga) are significantly longer than the timescales of deposition, and many of the concentration measurements will be qualitative in nature. Further, extrapolation will be difficult unless the size of the lake above the floor of Gale Crater can be estimated and compared to estimates of the contemporaneous global reservoir. That said, even qualitative information on the Fe-oxide deposition rate and its evolution over time would be useful. This could lead to order-of-magnitude inferences on the Fe flux from the subsurface, and the rate at which the mantle was being oxidized through Fe-oxide burial.

7. Conclusions

The idea that early Mars was warm and wet for prolonged time intervals, millions of years or more, is consistent with new data from the MSL mission. The only published mechanism that appears capable of maintaining such conditions for extended periods is the greenhouse effect of a $\text{CO}_2\text{-H}_2$ atmosphere. About 3 bar of CO_2 and 5 percent or more H_2 is required to produce global mean surface temperatures above freezing. Maintaining H_2 at this level is challenging but does not appear to be out of the question. Direct volcanic outgassing of H_2 from a highly reduced early martian mantle was probably the largest source of H_2 . Recycling of volatiles between the surface and the interior, as happens on Earth because of plate tectonics, would likely have been needed to provide this H_2 , as rates of juvenile outgassing are small. Additional H_2 could have been provided by photochemical oxidation of outgassed CH_4 and H_2S and by processes such as serpentinization and deposition of banded iron-formations. However, none of these sources are sufficient unless: i) the ancient Martian mantle was significantly more reduced than today, ii) volcanic outgassing rates were substantially

higher than those on modern Earth or iii) hydrogen escaped to space more slowly than the diffusion limit. Some combination of these three mechanisms could also work.

Recycling of water through the mantle followed by outgassing of H_2 should have oxidized the mantle over time. Such oxidation is consistent with the observed spread in $f\text{O}_2$ values of SNC meteorites from as low as IW-1 up to near QFM. Additional tests of the H_2 greenhouse hypothesis may be provided by MSL and by future missions. MSL itself could look for evidence of banded iron-formations and changes in D/H ratios that might indicate hydrogen loss, as well as providing qualitative and contextual information on the redox evolution of the martian mantle. Future sample return missions could look for quantitative evidence of secular mantle oxidation over time. Improved numerical models of hydrodynamic escape could shed light on the escape rate of H over time. Additional 3-D climate modeling work would also be useful to better constrain the amounts of rainfall and surface runoff that could have been maintained by this model and by its competitors, and compare these results to the lacustrine and fluvial deposits in Gale Crater and across the planet.

Acknowledgements

This material is based upon work supported by the National Science Foundation under Grant No. DGE1255832 to N. Batalha. Any opinions, findings, and conclusions or recommendations expressed in this material are those of the author(s) and do not necessarily reflect the views of the National Science Foundation. JFK acknowledges support from NASA's Exobiology and Astrobiology programs. R.R. acknowledges support from the Simon's Foundation (SCOL 290357, L.K.) and the Carl Sagan Institute.

References

- Anguita, F. et al., 2001. Tharsis dome, Mars: New evidence for Noachian-Hesperian thick-skin and Amazonian thin-skin tectonics. *Journal of Geophysical Research*, 106, p.7577.
- Braterman, P.S., Cairns-Smith, A.G. & Sloper, R.W., 1983. Photooxidation of hydrated Fe^{+2} -- significance for banded iron formations. *Nature*, 303, pp.163–164.
- Buser, M. et al., 2004. Far-infrared absorption by collisionally interacting nitrogen and methane molecules. *The Journal of chemical physics*, 121(6), pp.2617–21. Available at: <http://www.ncbi.nlm.nih.gov/pubmed/15281860> [Accessed October 15, 2014].

- Byrne, B. & Goldblatt, C., 2014. Radiative forcings for potential Archean greenhouse gases. *Climate of the Past*, 10, pp.2011–2053.
- Carter, J. et al., 2013. Widespread surface weathering on early Mars: a case for a warmer and wetter Mars. In *44th LPSC*. p. 1755.
- Chassefière, E. et al., 2014. Serpentinization as a possible mechanism at the origin of valley network formation on early Mars. In *AGU Fall Meeting*. p. P53C–4025.
- Connerney, J.E., 1999. Magnetic Lineations in the Ancient Crust of Mars. *Science*, 284, pp.794–798.
- Craddock, R.A. & Greeley, R., 2009. Minimum estimates of the amount and timing of gases released into the martian atmosphere from volcanic eruptions. *Icarus*, 204, pp.512–526.
- Von Damm, K.L., 2000. Chemistry of hydrothermal vent fluids from 9°–10°N, East Pacific Rise: “Time zero,” the immediate post-eruptive period. *Journal of Geophysical Research*, 105, p.11203.
- Von Damm, K.L., 1995. Controls on the chemistry and temporal variability of seafloor hydrothermal fluids. In *Seafloor Hydrothermal Systems: Physical, Chemical, Biological, and Geological Interactions*. pp. 222–247. Available at: <http://dx.doi.org/10.1029/GM091p0222>.
- Le Deit, L. et al., 2012. Extensive surface pedogenic alteration of the Martian Noachian crust suggested by plateau phyllosilicates around Valles Marineris. *Journal of Geophysical Research E: Planets*, 117.
- Domagal-Goldman, S.D. et al., 2014. Abiotic Ozone and Oxygen in Atmospheres Similar To Prebiotic Earth. *The Astrophysical Journal*, 792(2), p.90. Available at: <http://stacks.iop.org/0004-637X/792/i=2/a=90?key=crossref.6164bb734b270ea582854b1aa313d3d7> [Accessed September 15, 2014].
- Domagal-Goldman, S.D. et al., 2011. Using biogenic sulfur gases as remotely detectable biosignatures on anoxic planets. *Astrobiology*, 11(5), pp.419–41. Available at: <http://www.pubmedcentral.nih.gov/articlerender.fcgi?artid=3133782&tool=pmcentrez&rendertype=abstract> [Accessed September 16, 2014].
- Ehlmann, B.L. et al., 2009. Identification of hydrated silicate minerals on Mars using MRO-CRISM: Geologic context near Nili Fossae and implications for aqueous alteration. *Journal of Geophysical Research E: Planets*, 114.
- Farley, K. a et al., 2014. In situ radiometric and exposure age dating of the martian surface. *Science*, 343, p.1247166. Available at: <http://www.ncbi.nlm.nih.gov/pubmed/24324273>.
- Fassett, C.I. & Head, J.W., 2008. The timing of martian valley network activity: Constraints from buffered crater counting. *Icarus*, 195, pp.61–89.
- Forget, F. et al., 2013. 3D modelling of the early martian climate under a denser CO₂ atmosphere: Temperatures and CO₂ ice clouds. *Icarus*, 222, pp.81–99.
- Fox, J.L., 1993. The Production and Escape of Nitrogen-Atoms on Mars. *Journal of Geophysical Research-Planets*, 98, pp.3297–3310. Available at: <Go to ISI>://A1993KX58700018.
- Franz, H.B. et al., 2014. Isotopic links between atmospheric chemistry and the deep sulphur cycle on Mars. *Nature*, 508(7496), pp.364–8. Available at: <http://www.ncbi.nlm.nih.gov/pubmed/24740066> [Accessed October 15, 2014].
- Frost, D., Lee, J.H.S. & Ciccarelli, G., 1991. The use of Hugoniot analysis for the propagation of vapor explosion waves. *Shock Waves*, 1(2), pp.99–110.
- Frost, D.J. & McCammon, C.A., 2008. The Redox State of Earth’s Mantle. *Annual Review of Earth and Planetary Sciences*, 36, pp.389–420.
- Gaillard, F. & Scaillet, B., 2009. The sulfur content of volcanic gases on Mars. *Earth and Planetary Science Letters*, 279(1-2), pp.34–43.
- Gaudin, A., Dehouck, E. & Mangold, N., 2011. Evidence for weathering on early Mars from a comparison with terrestrial weathering profiles. *Icarus*, 216, pp.257–268.
- Grott, M. et al., 2013. Long-term evolution of the martian crust-mantle system. *Space Science Reviews*, 174(1-4), pp.49–111. Available at: <http://link.springer.com/10.1007/s11214-012-9948-3> [Accessed September 16, 2014].

- Grott, M. et al., 2011. Volcanic outgassing of CO₂ and H₂O on Mars. *Earth and Planetary Science Letters*, 308, pp.391–400.
- Grotzinger, J.P. et al., 2013. A Habitable Fluvio-Lacustrine Environment at Yellowknife Bay, Gale Crater, Mars. *Science (New York, N.Y.)*, 343, pp.1–18. Available at: <http://www.ncbi.nlm.nih.gov/pubmed/24324272>.
- Halevy, I. & Head III, J.W., 2014. Episodic warming of early Mars by punctuated volcanism. *Nature Geoscience*, 2(November), pp.2–5. Available at: <http://www.nature.com/doi/10.1038/ngeo2293> [Accessed November 18, 2014].
- Halmer, M.M., Schmincke, H.U. & Graf, H.F., 2002. The annual volcanic gas input into the atmosphere, in particular into the stratosphere: A global data set for the past 100 years. *Journal of Volcanology and Geothermal Research*, 115, pp.511–528.
- Hoke, M.R.T., Hynek, B.M. & Tucker, G.E., 2011. Formation timescales of large Martian valley networks. *Earth and Planetary Science Letters*, 312, pp.1–12.
- Holland, H.D., 1973. The oceans: a possible source of iron in iron-formations. *Econ. Geol.*, 68, pp.1169–1172.
- Holland, H.D., 2002. Volcanic gases, black smokers, and the great oxidation event. *Geochimica et Cosmochimica Acta*, 66, pp.3811–3826.
- Holland, H.D., 2009. Why the atmosphere became oxygenated: A proposal. *Geochimica et Cosmochimica Acta*, 73, pp.5241–5255.
- Holland, H.D. & Trendall, A.F., 1985. Earth History. *Science*, 227(4688), p.745.
- Hunten, D.M., Pepin, R.O. & Walker, J.C.G., 1987. Mass fractionation in hydrodynamic escape. *Icarus*, 69, pp.532–549.
- Hurowitz, J.A. et al., 2010. Origin of acidic surface waters and the evolution of atmospheric chemistry on early Mars. *Nature Geoscience*, 3, pp.323–326.
- Irwin, R.P., Howard, A.D. & Craddock, R.A., 2008. Fluvial Valley Networks on Mars. In *River Confluences, Tributaries and the Fluvial Network*. pp. 419–451.
- Jarrard, R.D., 2003. Subduction fluxes of water, carbon dioxide, chlorine, and potassium. *Geochemistry, Geophysics, Geosystems*, 4.
- Kasting, J.F., 1991. CO₂ condensation and the climate of early Mars. *Icarus*, 94, pp.1–13.
- Kasting, J.F., 1993. Earth's early atmosphere. *Science (New York, N.Y.)*, 259, pp.920–926.
- Kasting, J.F., 2010. *How to Find a Habitable Planet*, New Jersey: Princeton University Press.
- Kasting, J.F., 2013. What caused the rise of atmospheric O₂? *Chemical Geology*, 362, pp.13–25.
- Kasting, J.F. & Canfield, D.E., 2012. The Global Oxygen Cycle. In *Fundamentals of Geobiology*. pp. 93–104.
- Kasting, J.F., Liu, S.C. & Donahue, T.M., 1979. Oxygen Levels in the Prebiological Atmosphere that the large amount of oxygen. *Journal of Geophysical Research*, 84(9), pp.1–11.
- Kasting, J.F., Zahnle, K.J. & Walker, J.C.G., 1983. Photochemistry of Methane in the Earth's Early Atmosphere. *Developments in Precambrian Geology*, 7, pp.13–40.
- Kharecha, P., Kasting, J. & Siefert, J., 2005. A coupled atmosphere-ecosystem model of the early Archean earth. *Geobiology*, 3, pp.53–76.
- Kite, E. et al., 2013. Seasonal melting and the formation of sedimentary rocks on Mars, with predictions for the Gale Crater mound. *Icarus*, 223(1), pp.181–210.
- Koeppen, W.C. & Hamilton, V.E., 2008. Global distribution, composition, and abundance of olivine on the surface of Mars from thermal infrared data. *Journal of Geophysical Research*, 113(E0).
- Krasnopolsky, V.A., Mumma, M.J. & Gladstone, G.R., 1998. Detection of atomic deuterium in the upper atmosphere of Mars. *Science (New York, N.Y.)*, 280, pp.1576–1580.
- Kurokawa, H. et al., 2014. Evolution of water reservoirs on Mars: Constraints from hydrogen isotopes in martian meteorites. *Earth and Planetary Science Letters*, 394, pp.179–185.

- Lécuyer, C. & Ricard, Y., 1999. Long-term fluxes and budget of ferric iron: implication for the redox states of the Earth's mantle and atmosphere. *Earth and Planetary Science Letters*, 165(2), pp.197–211.
- Loizeau, D. et al., 2010. Stratigraphy in the Mawrth Vallis region through OMEGA, HRSC color imagery and DTM. *Icarus*, 205, pp.396–418.
- Mahaffy, P.R. et al., 2015. The imprint of atmospheric evolution in the D/H of Hesperian clay minerals on Mars. *Science*, 347(6220), pp.412–414.
- McSween, H.Y. et al., 2006. Characterization and petrologic interpretation of olivine-rich basalts at Gusev Crater, Mars. *Journal of Geophysical Research E: Planets*, 111.
- Meunier, A. et al., 2012. Magmatic precipitation as a possible origin of Noachian clays on Mars. *Nature Geoscience*, 5, pp.739–743.
- Michalski, J.R. & Niles, P.B., 2010. Deep crustal carbonate rocks exposed by meteor impact on Mars. *Nature Geoscience*, 3, pp.751–755.
- Montesi, L.G. & Zuber, M., 2003. Clues to the lithospheric structure of Mars from wrinkle ridge sets and localization instability. *Journal of Geophysical Research*, 108(5048).
- Noe Dobrea, E.Z. et al., 2010. Mineralogy and stratigraphy of phyllosilicate-bearing and dark mantling units in the greater Mawrth Vallis/west Arabia Terra area: Constraints on geological origin. *Journal of Geophysical Research: Planets*, 115(E7).
- Pavlov, A.A. & Kasting, J.F., 2002. Mass-independent fractionation of sulfur isotopes in Archean sediments: strong evidence for an anoxic Archean atmosphere. *Astrobiology*, 2, pp.27–41.
- Pollack, J.B. et al., 1987. The case of a wet, warm climate on early Mars. *Icarus*, 71(2), pp.203–224.
- Poulet, F. et al., 2005. Phyllosilicates on Mars and implications for early martian climate. *Nature*, 438, pp.623–627.
- Ramirez, R.M. et al., 2014. Warming early Mars with CO₂ and H₂. *Nature Geoscience*, 7(1), pp.59–63. Available at: <http://www.nature.com/doi/10.1038/ngeo2000> [Accessed September 16, 2014].
- Righter, K. et al., 2008. Oxygen fugacity in the Martian mantle controlled by carbon: New constraints from the nakhlite MIL 03346. *Meteoritics & Planetary Science*, 43, pp.1709–1723. Available at: <http://dx.doi.org/10.1111/j.1945-5100.2008.tb00638.x>.
- Segura, A. et al., 2003. Ozone concentrations and ultraviolet fluxes on Earth-like planets around other stars. *Astrobiology*, 3, pp.689–708.
- Segura, T.L. et al., 2002. Environmental effects of large impacts on Mars. *Science (New York, N.Y.)*, 298, pp.1977–1980.
- Segura, T.L., McKay, C.P. & Toon, O.B., 2012. An impact-induced, stable, runaway climate on Mars. *Icarus*, 220, pp.144–148.
- Segura, T.L., Toon, O.B. & Colaprete, A., 2008. Modeling the environmental effects of moderate-sized impacts on Mars. *Journal of Geophysical Research*, 113(E11).
- Sleep, N.H., 2005. Evolution of the continental lithosphere. *Annual Review of Earth and Planetary Sciences*, 33, pp.369–393. Available at: <Go to ISI>://000229840700013.
- Sleep, N.H., 1994. Martian plate tectonics. *Journal of Geophysical Research*, 99, pp.5639–5655.
- Stanley, B.D., Hirschmann, M.M. & Withers, A.C., 2011. CO₂ solubility in Martian basalts and Martian atmospheric evolution. *Geochimica et Cosmochimica Acta*, 75, pp.5987–6003.
- Tian, F. et al., 2014. High stellar FUV/NUV ratio and oxygen contents in the atmospheres of potentially habitable planets. *Earth and Planetary Science Letters*, 385, pp.22–27. Available at: <http://linkinghub.elsevier.com/retrieve/pii/S001221X13005876> [Accessed September 18, 2014].
- Tian, F. et al., 2010. Photochemical and climate consequences of sulfur outgassing on early Mars. *Earth and Planetary Science Letters*, 295, pp.412–418.
- Tian, F., Kasting, J.F. & Solomon, S.C., 2009. Thermal escape of carbon from the early Martian atmosphere. *Geophysical Research Letters*, 36.

- Urata, R.A. & Toon, O.B., 2013. A new general circulation model for Mars based on the NCAR Community Atmosphere Model. *Icarus*, 226(1), pp.336–354.
- Wade, J. & Wood, B.J., 2005. Core formation and the oxidation state of the Earth. *Earth and Planetary Science Letters*, 236, pp.78–95.
- Warren, P. & Gregory, K., 1996. Siderophile trace elements in ALH84001, other SNC meteorites and eucrites: Evidence of heterogeneity, possibly time-linked, in the mantle of Mars. *Meteoritics & Planetary Science*, 31(1), pp.97–105.
- Wetzel, D.T. et al., 2013. Degassing of reduced carbon from planetary basalts. *Proceedings of the National Academy of Sciences of the United States of America*, pp.3–6. Available at: <http://www.ncbi.nlm.nih.gov/pubmed/23569260>.
- Wordsworth, R. et al., 2013. Global modelling of the early Martian climate under a denser CO₂ atmosphere: Water cycle and ice evolution. *Icarus*, 222(1), pp.1–19.
- Wordsworth, R., Forget, F. & Eymet, V., 2010. Infrared collision-induced and far-line absorption in dense CO₂ atmospheres. *Icarus*, 210, pp.992–997.
- Wordsworth, R. & Pierrehumbert, R., 2013. Hydrogen-nitrogen greenhouse warming in Earth's early atmosphere. *Science (New York, N.Y.)*, 339, pp.64–7. Available at: <http://www.ncbi.nlm.nih.gov/pubmed/23288536>.
- Zahnle, K.J., 1986. Photochemistry of methane and the formation of hydrocyanic acid (HCN) in the Earth's early atmosphere. *Journal of Geophysical Research*, 91(D2), p.2819. Available at: <http://doi.wiley.com/10.1029/JD091iD02p02819>.